PWM Based Fixed Frequency Equivalent SM Controller for Stability of DC Microgrid System

DOI : 10.36909/jer.ICEPE.19465

Muhammad Rashad*, Uzair Raoof**,Nazam Siddique***, Ghulam Abbas****, Bilal Ashfaq Ahmed*****

*,**,****,*****Department of Electrical Engineering, The University of Lahore (UOL), Lahore 54000, Pakistan.

***,Department of Electrical Engineering, University of Gujrat (UOG), Gujrat 50700, Pakistan.

* Corresponding Author: ghulam.abbas@ee.uol.edu.pk

ABSTRACT

DC microgrids are localized and independent power distribution networks which show high efficiency when batteries and renewable sources are interconnected with the system. This paper addresses the stability of the dc microgrid through a decentralized control scheme. A centralized control architecture can improve the stability but reliability is compromised if the central controller fails. Droop control is commonly used to address the stability problem based on techniques through linear controllers. However, the Droop controller requires a tradeoff between voltage regulation and droop gain. Further, the global stability of the systems cannot be ensured through linear control techniques. Additionally, for different operating requirements and load conditions, it is difficult to optimize the parameters of these controllers. To address limitations, a PWM Based fixed frequency equivalent sliding mode (SM) control technique is proposed for dc microgrid stability. SM controllers show high robust performance. To formulate the problem, system equations are modeled and the operation of the system under SM is verified for existence and stability conditions. To examine the transient performance, the responses for critically damped and underdamped are investigated and presented. The results of detailed experiments simulations are presented which show the efficiency of the proposed control method.

Keywords: Microgrid; droop controller; equivalent sliding mode controller; existence condition; underdamped; critically damped.

INTRODUCTION

The distribution power network is the end-stage of the electrical power system. It transmits power from the transmission network to the end-user. Power losses in the low voltage ac distribution system and domestic appliances are a hot issue in the growing energy concerns. Due to the increased dependence on renewable sources in the power distribution network and a shift of domestic appliances from ac to dc, attracting dc distribution for power delivery to end-user. Most of the domestic and commercial appliances directly or indirectly run on dc power. Thus, the dc distribution can be more efficient compared to ac distribution (Techakittiroj et al., 2009, Rashad et al. 2018 & Rashad et al. 2018).

Dc microgrids are gaining popularity in housing and commercial buildings and data centers. The efficiency of dc microgrids is expected to be increased by 10-22% compared to ac microgrids (Becker, D. & Sonnenberg, B. 2011). Furthermore, in dc power distribution, the circuits for frequency synchronization and reactive power compensation are no more required which have a key role in ac systems. Due to these concerns, the subject of dc microgrids is attracting researchers. However, dc microgrids are not exempted from stability issues. Particularly the stability issues while connecting the PE converter-based tightly regulated Constant Power Loads (CPLs) which are more prone to small signal instabilities (Hassan, M. A. & He, Y. 2020). Any change in voltage applied to the CPL will change the load current. This leads to unstable coordination among sources and load subject to a small perturbation in the system. To address the problem, the solution proposed in distribution (Cespedes et al., 2011) is based on passive filters which are bulky and lossy. Other solutions proposed in the literature to stabilize dc microgrids are based on coordination Generally, the control scheme to coordinate among different elements in microgrids is classified into centralized and decentralized architectures. In a centralized scheme, a microgrid using a high bandwidth channel communicates system information with a single central controller which interprets the collected information, schedules the tasks, and directs the PE converters about the decisions (Rashad et al. 2018, Rashad et al. 2018, Meng et al. 2017 & Shivam & Dahiya, R. 2017). However, if a single central controller fails, the reliability is compromised. Whereas in a decentralized scheme, PE converters operate on local droop controllers based on measured physical quantities (Rashad et al. 2018, Rashad et al. 2018, Meng et al. 2017 & Shivam & Dahiya, R. 2017). Significant advantages are low cost and relaxed scalability. However, Droop controllers introduce large voltage deviations in dc buses due to large droop values which are required for a wide stability margin. Therefore, some modified droop control based on distributive control architecture is essential to control dc grids. In (Ghalebani, P. & Niasati, M.

2018 & Anand et al. 2013), a distributive scheme is proposed which adapts the droop gain against the changes in load conditions through a communication channel of low bandwidth. In (Nasirian et al. 2015), a cooperative distributive droop control using an integral action is proposed for power-sharing and voltage stability. Similar integral action for a team-oriented power-sharing control among dc to dc converters is proposed in (Moayedi et al. 2015). For communication among the microgrid elements, graph theory and multi-agent type approaches are presented in (Behjati et al. 2014 & Morstyn et al. 2016). However, approaches based on distributive control require high computational devices and suffer the convergence speed which is affected due to the communication delays.

The control of PE converters in each source is mostly designed using linearized control techniques which show limited operations and the global stability cannot have ensured at the desired equilibrium point (Anand et al. 2013, Karlsson, P. 2002 & Mahmoodi et al. 2006). The controller parameters for different operating requirements and load conditions cannot be optimized for these controllers. In addition, they exhibit slower transient responses. Moreover, renewable sources heavily rely on environmental conditions. Therefore, it is difficult for conventional control techniques to maintain stability during the sudden change in generation and load conditions. Therefore, system stability is a key problem in dc microgrids.

Due to the nonlinear nature of the PE converters, the nonlinear control techniques seek a great concern regarding the stability and coordination in a microgrid application. Therefore, a hybrid model predictive control (MPC) technique is proposed in (Dragicevic, T. 2018) for a PE converter. But, due to the high computational requirements, MPC for practical implementation is not attractive. The controllers based on the passivity approach are also employed in literature for PE converters (Hassan, M. A. & He, Y. 2020). However, high accuracy of the model is required in these controllers which motivates the design of controllers through easy modeling and simple implementation. In (Fadil, H. E. & Giri, F. 2007), a controller based on a back-stepping approach is applied to PE converters subject to stabilization and tracking problems. However, this technique is reported only for restive loads. Alternatively, a nonlinear sliding mode control (SMC) technique using a hysteresis relay is proposed in (Rashad et al. 2018, Yasin et al., 2021 & Rashad et al. 2018). Switching action using hysteresis relay generates an average non-zero value for which voltage error cannot be eliminated. Further, switching frequency through hysteresis control suffers a problem with variation in frequency (Spiazzi, G. & Mattavelli, P. 2002).

In (Dominguez et al. 2016), cascaded voltage and current loops are proposed to control the PE converter subject to voltage and current tracking. The voltage loop is designed using a

traditional PI controller and the current loop uses an SMC technique. This control method suffers a problem of transient performance. Another SMC technique proposed in (Etxeberria et al. 2011) is to control the PE bidirectional converter for hybrid management of batteries. A duty cycle variation is a problem in this method that prevents its implementation.

To address the limitations, a PWM Based fixed frequency equivalent SM control technique is proposed in this paper for stability and transient performance. This paper aims to contribute the following points:

- The formulation of problem and modeling of system equations.
- To ensure the SM operation, hitting and existence conditions of the modeled system are verified. Additionally, the equation of equivalent SM controller to map with PWM function is developed for dc to dc converters.
- The stability condition of the dc microgrid system under SM operation is analyzed and verified, and the system response for the different transient conditions is presented.
- To validate the performance, the results of detailed experiments simulations are presented.

MODELING OF SYSTEM EQUATIONS

A generalized configuration of a dc microgrid system is shown in Fig. 1. The PE converters (dc to dc, dc to ac, etc.) are required to interconnect elements with dissimilar characteristics. To exchange power, the microgrids can be interconnected with the main utility grid or other ac and dc microgrids. A one-source model connected with the dc microgrid is shown in Fig. 2. The source voltage is modeled as v_i with source current as i_s, whereas, the output voltage and associated connecting line are represented as v_o and R_{line} respectively. The differential equations of the modeled system are given in (1) and (2).

$$\frac{dv_o}{dt} = \frac{i_L - i_R - i}{C} \tag{1}$$

$$\frac{di_L}{dt} = \frac{-v_o + uv_i}{L} \tag{2}$$

Where, i_L, i_R, i, C and L are inductor current, load current, connecting line current, capacitance and inductance respectively. While u represents the state of power switch Q.

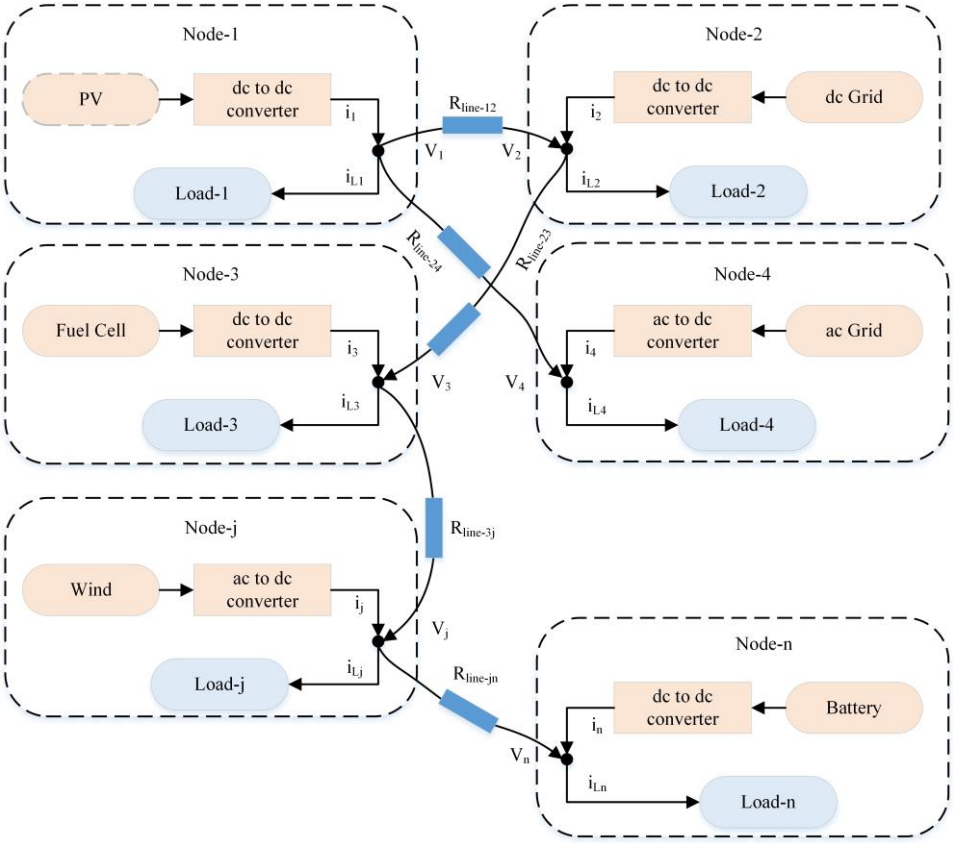

Figure 1. DC microgrid system

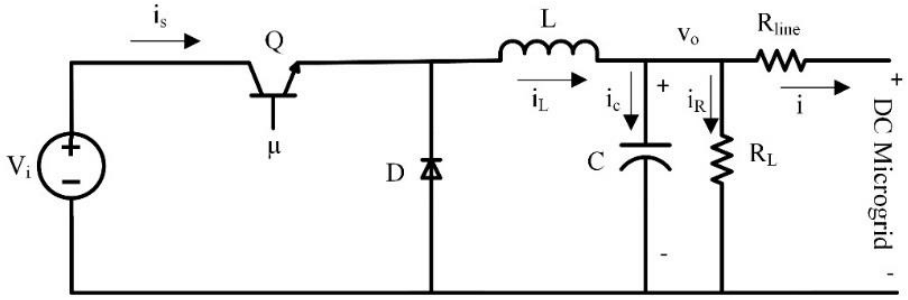

Figure 2. One source model with dc microgrid

$$x_1 = V_{ref} - \beta v_o \qquad (4a)$$

Differentiating (4a) results in a rate of change of voltage error x_2 as

$$x_2 = \frac{d(V_{ref} - \beta v_o)}{dt} = -\beta \frac{dv_o}{dt} = -\frac{\beta}{C} i_c \qquad (4b)$$

and

$$x_3 = \int (V_{ref} - \beta v_o) dt \qquad (4c)$$

Where V_{ref} and β are reference voltage and sensing ratio respectively. To represent the system in state-space form, differentiating (4a) and (4b) results as

$$\dot{x_1} = \frac{d}{dt}(x_1) = -\beta_j \frac{dv_j}{dt} = x_2 \qquad (5a)$$

$$\dot{x_2} = -\frac{\beta}{C}\left(\frac{di_c}{dt}\right) \qquad (5b)$$

Substituting (1) and (2) in (5b) results in a simplified form as

$$\dot{x_2} = -\frac{1}{R_L C}x_2 - \frac{\beta}{LC}v_i u + \frac{\beta}{LC}v_o + \frac{\beta}{C}\left(\frac{di}{dt}\right) \qquad (5c)$$

In steady-state conditions, considering the constant voltage drop across the line R_{line} will result $\frac{di}{dt} = 0$. Substituting this value in (5c) results as

$$\dot{x_2} = -\frac{1}{R_L C}x_2 - \frac{\beta}{LC}v_i u + \frac{\beta}{LC}v_o \qquad (5d)$$

Now differentiating (4c) results as

$$\dot{x_3} = V_{ref} - \beta v_o = x_1 \qquad (5e)$$

From (5a), (5d), and (5e), the dynamics of the system in the state-space form are expressed in (6).

$$\begin{pmatrix} \dot{x_1} \\ \dot{x_2} \\ \dot{x_3} \end{pmatrix} = \begin{pmatrix} 0 & 1 & 0 \\ 0 & -\frac{1}{R_L C} & 0 \\ 1 & 0 & 0 \end{pmatrix} \begin{pmatrix} x_1 \\ x_2 \\ x_3 \end{pmatrix} + \begin{pmatrix} 0 \\ -\frac{\beta v_i}{LC} \\ 0 \end{pmatrix} u + \begin{pmatrix} 0 \\ \frac{\beta v_o}{LC} \\ 0 \end{pmatrix} \qquad (6)$$

The system dynamics in (6) are used for the stability and design of the controller.

SLIDING MODE ANALYSIS

After modeling the system in (6), next is to analyze the existence and stability of the SM controller. In PE converters, the control law u which is used to adapt the switching action is generally expressed as

$$u = \begin{cases} 1 & when\ \Psi > 0 \\ 0 & when\ \Psi < 0 \end{cases} \qquad (7)$$

Where Ψ is a sliding surface that defines the instantaneous system trajectories. The control law defined in (7) is the basic requirement of the hitting condition of a system under SM. This law will force the system trajectories will reach finally the sliding manifold Ψ.

In most SM controllers, one or more error states are included in the sliding surface design (Zhao et al. 2014). In this paper, a sliding surface is proposed which includes an error, rate of change of error, and integral of error in sliding. This makes it a proportional, derivative, and integral type SM controller. The proposed sliding surface is expressed as

$$\Psi = \alpha_1 x_1 + \alpha_2 x_2 + \alpha_3 x_3 \qquad (8)$$

Where $x_1, x_2, and\ x_3$ are state variables of voltage, rate of change, and integral of voltage errors respectively. Whereas, $\alpha_1, \alpha_2, and\ \alpha_3$ represent the sliding coefficients of the SM controller. The diagram representing the sliding surface Ψ is shown in Fig. 3.

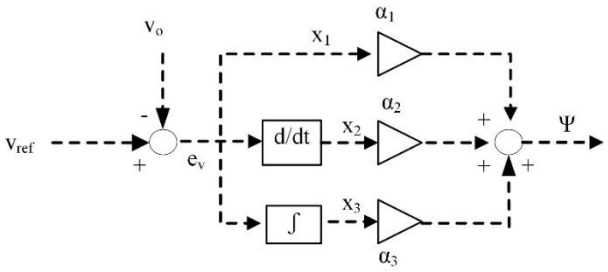

Figure 3. Sliding surface Ψ

the derivative of sliding surface Ψ is can be expressed as

$$\frac{d\Psi}{dt} = -\alpha_1 \frac{\beta i_c}{C} + \alpha_2 \frac{\beta i_c}{R_L C^2} + \alpha_3 (V_{ref} - \beta v_o) - \alpha_2 \frac{\beta v_i}{LC} u + \alpha_2 \frac{\beta v_o}{LC} \qquad (9)$$

The equation in (9) is further used to validate the existence of the SM controller,

CONTROLLABILITY CONDITION

The controllability condition defines whether the system under SM is controllable or not. This condition is the basic requirement to check the sliding surface Ψ such that the system is controllable through the control variable (Spiazzi, G. & Mattavelli, P. 2002) and is defined as

$$\frac{d}{du}\left(\frac{d\Psi}{dt}\right) \neq 0 \qquad (10)$$

Substituting (9) into (10) results as

$$\frac{d}{du}\left(\frac{d\Psi}{dt}\right) = -\alpha_2 \frac{\beta}{LC}(v_i) \neq 0 \qquad (11)$$

The (11) depends on the value of α_2. To guarantee the condition in (11), α_2 must not be selected as zero value. Further, $\beta, L, C\ and\ v_i$ are positive quantities. Hence (11) will be satisfied and the system will be controllable.

EXISTENCE CONDITION

To ensure that the SM operation will exist and system trajectories remain within the vicinity of sliding manifold Ψ, the existence condition must be obeyed which satisfies the asymptotic stability requirement (Utkin et al. 1999). This condition is well-defined as

$$\lim_{\Psi \to 0} \Psi . \dot{\Psi} < 0 \qquad (12)$$

Case-1: in (12), as $\Psi \to 0^+$ ($u = 1, \& \dot{\Psi} < 0$), Substituting the value of $\dot{\Psi}$ it can be expressed as

$$-\beta L \left(\frac{\alpha_1}{\alpha_2} - \frac{1}{R_L C}\right) i_c + \frac{\alpha_3}{\alpha_2} LC\left(V_{ref} - \beta v_o\right) + \beta v_o - \beta v_i < 0 \qquad (13)$$

Case-2: in (21), as $\Psi \to 0^-(u = 0, \& \dot{\Psi} > 0)$, it can be expressed as

$$-\beta L \left(\frac{\alpha_1}{\alpha_2} - \frac{1}{R_L C}\right) i_c + \frac{\alpha_3}{\alpha_2} LC\left(V_{ref} - \beta v_o\right) + \beta v_o > 0 \qquad (14)$$

Combining (13) and (14), the expression for existence condition can be represented as

$$0 < -\beta L \left(\frac{\alpha_1}{\alpha_2} - \frac{1}{R_L C}\right) i_c + \frac{\alpha_3}{\alpha_2} LC\left(V_{ref} - \beta v_o\right) < \beta (v_o - v_i) \qquad (15)$$

Satisfying (15) will ensure the SM operation and system's trajectories will follow the desired response. Failing to satisfy (15) may result that the trajectories moving away from the sliding manifold which is not desired.

PWM BASED EQUIVALENT CONTROL

There are two types of SM controller implementation. A conventional method of design is through a hysteresis modulation-based controller. The hysteresis band creates an average non-zero value which cannot eliminate the voltage error. Further, the hysteresis unction suffers a problem with switching frequency variation. These drawbacks can be addressed using a PWM-based equivalent controller. The equivalent control u_{eq} is derived by putting $\dot{\Psi} = 0$ and the simplified result can be expressed as

$$0 < {u_{eq}}^* = -\beta L \left(\frac{\alpha_1}{\alpha_2} - \frac{1}{R_L C}\right) i_c + \frac{\alpha_3}{\alpha_2} LC\left(V_{ref} - \beta v_o\right) + \beta v_o < \beta v_i \qquad (16)$$

Where u_{eq} is continuous and bounded by inequality as $0 < u_{eq} < 1$. To transform the control function in (16) into duty ratio d of PWM, where $0 < d = \frac{v_c}{v_{ramp}} < 1$, can be expressed as

$$v_c = {u_{eq}}^* = -\beta L \left(\frac{\alpha_1}{\alpha_2} - \frac{1}{R_L C}\right) i_c + \frac{\alpha_3}{\alpha_2} LC\left(V_{ref} - \beta v_o\right) + \beta v_o \qquad (17)$$

Where $v_c \; and \; v_{ramp} = \beta v_i$ are control and ramp signals required to generate the duty cycle of PWM. The (17) can be further simplified as

$$v_c = {u_{eq}}^* = -K_{p1} i_c + K_{p2}\left(V_{ref} - \beta v_o\right) + \beta v_o \qquad (18)$$

Where, K_{p1} and K_{p2} are gains required to calculate the feedback control signals v_c. Gains K_{p1} and K_{p2} are calculated using $K_{p1} = \beta L\left(\frac{\alpha_1}{\alpha_2} - \frac{1}{R_L C}\right)$ and $K_{p2} = \frac{\alpha_3}{\alpha_2} LC$ respectively. The coefficients $\alpha_1, \alpha_2, and\ \alpha_3$, necessity be selected to fulfill the condition presented in (15).

STABILITY OF SLIDING COEFFICIENTS

The existence condition given in (26) guarantees the existence of SM operation. It does not give any information about the stability of sliding coefficients. To select and prove stability, Ackermann's formula is applied which naturally fulfills the stability requirements of these coefficients (Utkin et al. 1999). Sliding coefficients can be attained by putting $\Psi = 0$ which results as

$$\alpha_1 x_1 + \alpha_2 \frac{dx_1}{dt} + \alpha_3 \int x_1 = 0 \qquad (19)$$

Taking the derivative of (19) and rearranging gives as

$$\frac{d^2 x_1}{dt^2} + \left(\frac{\alpha_1}{\alpha_2}\right)\frac{dx_1}{dt} + \left(\frac{\alpha_3}{\alpha_2}\right) x_1 = 0 \qquad (20)$$

Comparing (20) with the standard second-order system's equation, undamped natural frequency ω_n and damping ratio ζ can be expressed as

$$\zeta = \frac{\alpha_1}{2\sqrt{\alpha_2 \alpha_3}}, \quad \omega_n = \sqrt{\frac{\alpha_3}{\alpha_2}}, \quad \& \quad \frac{\alpha_3}{\alpha_2} = \frac{1}{4\zeta^2}\left(\frac{\alpha_1}{\alpha_2}\right)^2 \qquad (21)$$

The coefficients $\alpha_1, \alpha_2, and\ \alpha_3$ can be selected to satisfy the desired transient performance.

EXPERIMENTS SIMULATION AND DISCUSSION

To examine the results and effectiveness of the proposed control scheme, a dc microgrid system interconnecting three-source and load as shown in Fig. 4 is simulated through MATLAB/Simulink. This type of microgrid configuration is feasible in remote areas where the main utility power grid is not easily extendable. Each source consists of a PE dc to dc converter with parameters shown in Table 1. The specifications of the dc microgrid system are given in Tables 2 and 3 respectively.

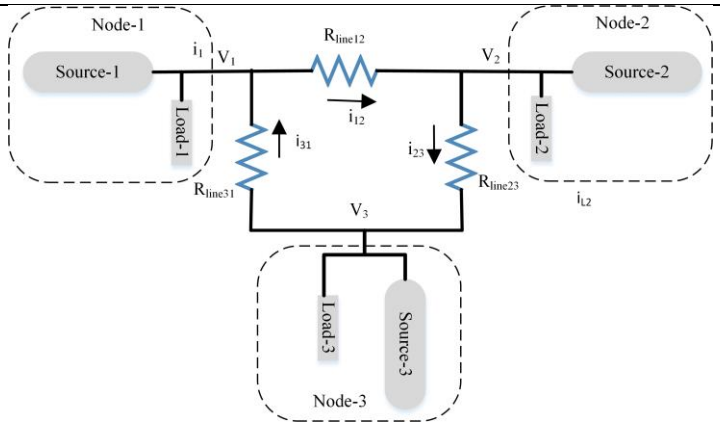

Figure 4. Three-source dc microgrid

Table 1. Parameters of PE converter

Parameters	Value
Voltage	400 V
Switching frequency	10 kHz
Inductor, L	100 µH
Capacitor, C	4000 µF

- Results through droop controller

The droop controller in each source is shown in Fig. 5. The dc microgrid system of Fig. 4 is simulated with 0.04Ω, 1.9Ω, and 0.4Ω droop gains, and node voltages are shown in Fig. 6. Observed voltage regulation at node 1, 2 and 3 are 1.6%, 4.9% and 6.9% respectively. This shows that voltage regulation requirements can be ensured with small droop values but the voltage regulation is not accepted with large droop values. Hence a voltage regulation tradeoff is needed.

Table 2. Parameters of each node

Parameters	Node-1	Node-2	Node-3
Nominal node voltage	400 V		
Rated source power	20 kW	50 kW	100 kW
Rated load power	10 kW	30 kW	60 kW
Droop gains	0.04 Ω	1.9 Ω	0.4 Ω
Voltage regulation	≤ ±3%		

Table 3. Connecting lines specifications

Parameters	Branch-12	Branch-23	Branch-31
Cable type	3-Conductor Al-PVC185mm^2		
Resistance (per meter)	0.152 m Ω		
Connecting line length	1000 meters	2000 meters	3000 meters

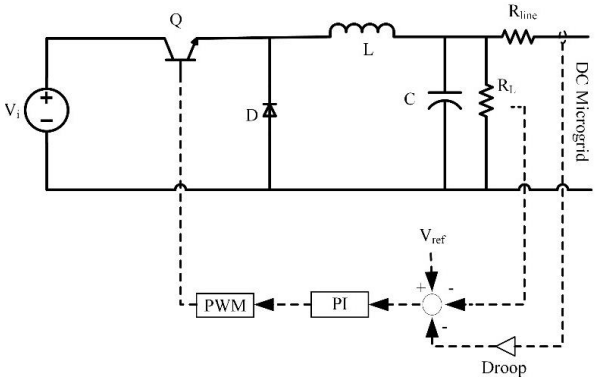

Figure 5. Droop controlled PE converter

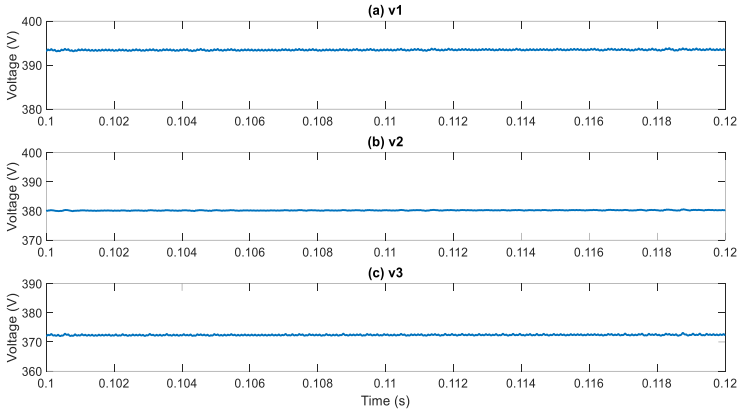

Figure 6. Node voltages with (a) droop 0.04 Ω (b) droop 1.9 Ω and (c) droop 0.4 Ω

- Results using sliding mode controller

The diagram of the PWM-based equivalent SM controller in each source is shown in Fig. 7. To observe the voltages at each node through the prosed controller, the simulated results are shown in Fig. 8. The maximum voltage regulation observed in this case is less than 1% which is a substantially lower value than the droop-controller. This shows the performance of an equivalent SM controller in a steady-state condition.

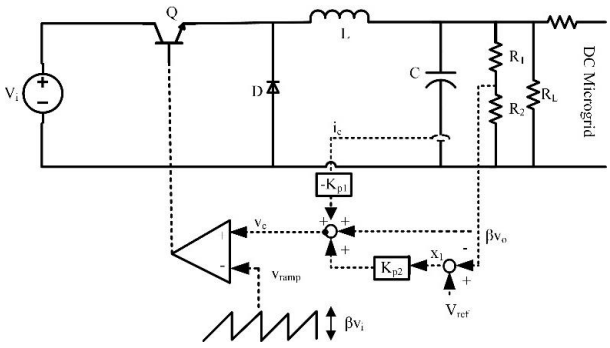

Figure 7. SM equivalent controlled PE converter

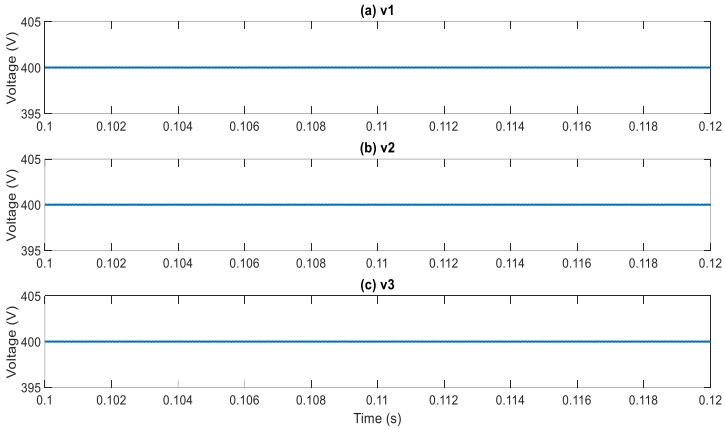

Figure 8. Node voltages with equivalent SM controller

To observe node voltages with source power variation, per unit (p.u.) power of sources is varied as shown in Fig. 9. Fig. 10 shows the voltages which confirm the efficiency of proposed technique with source power uncertainties.

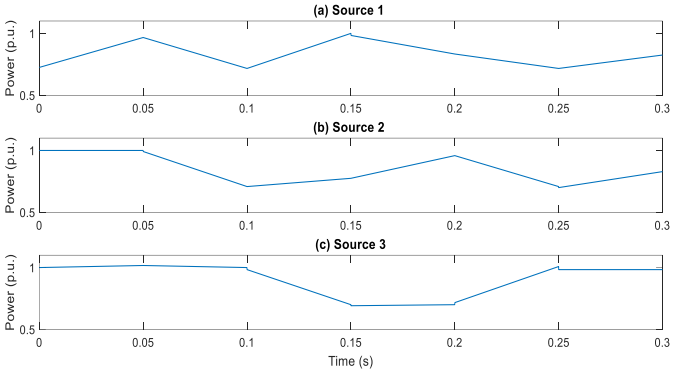

Figure 9. Source power variation per unit (p.u.)

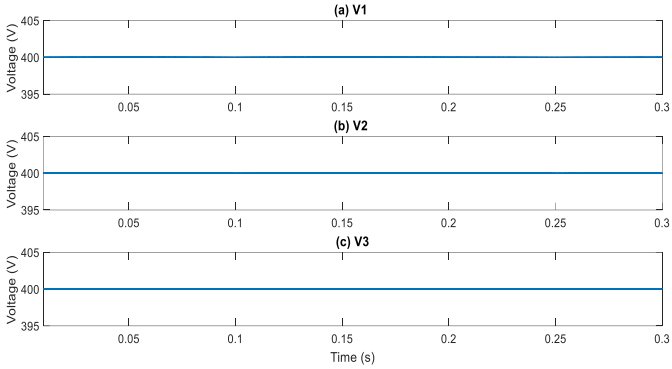

Figure 10. Voltages with source variation

For the transient performance, a step load is changed from 60 kW to 30 kW at 0.2s, and the simulated results are shown in Fig. 11. When the load is switched, a transient is produced which settles down to a steady-state in 4ms using droop control. Whereas, the observed settling time is 0.4ms using an equivalent controller which is a considerably small value than the droop-controller. Further, the observed overshoot using an equivalent controller is less than 1V which for droop control is 6V. This verifies the efficiency of the SM controller under transient conditions.

Furthermore, the transient is investigated for a critically damped and underdamped response. Fig. 12 shows the node voltage of a source when its load is switched from 100 kW to 60 kW at 0.2s with sliding coefficients which shows critically damped and underdamped responses. The results of transient parameters are summarized in Table 4. In an underdamped response, the response is improved with smaller values of overshoot and settling time as the value of damping ratio ζ is increased from 0.1 to 0.6. Further, the oscillations observed for $\zeta = 0.1$ are improved as the value of ζ is increased. These results are in good arrangement with the theory presented. Moreover for $\zeta = 1$, the response is critically damped in which overshoot, and settling time are further improved. These results verify the transient performance of the SM equivalent controller.

CONCLUSION

The modern form of power delivery to the consumers is a microgrid that can sufficiently generate energy and can share power with other microgrids and main utilities. DC microgrids are gaining popularity due to their high integration efficacy. The stability of the dc microgrid is a key stability concern The centralized control architecture for dc microgrids is not preferred because single-point failure can degrade the system reliability and performance. Droop control based on decentralized architecture needs a tradeoff between voltage regulation and droop gain. Further, the global stability of the systems cannot be ensured through linear control techniques.

Additionally, for different operating requirements and load conditions, it is hard to tune the parameters of these controllers. Therefore, these are not preferred for the stability of nonlinear systems. In this paper, a PWM-based SM controller is proposed for dc microgrid stability. The system is modeled and existence and stability conditions are verified for the SM operation. To examine the transient response, critically damped and underdamped responses are investigated and presented. The results of detailed experiments simulations are presented compared with the droop controller which shows the efficiency of the steady-state and transient performance proposed controller.

Table 4. Voltage response with different values of ζ

Damping ratio ζ	**Parameter K_{p1}, K_{p2}**	**Settling time**	**Response type**
$\zeta = 0.1$	9.98, 10^5	3.75 ms	Underdamped
$\zeta = 0.3$	9.98, 11.8× 10^3	1 ms	Underdamped
$\zeta = 0.6$	9.98, 2777.6	0.3 ms	Underdamped
$\zeta = 1$	9.98, 10^3	0.15 ms	Critically damped

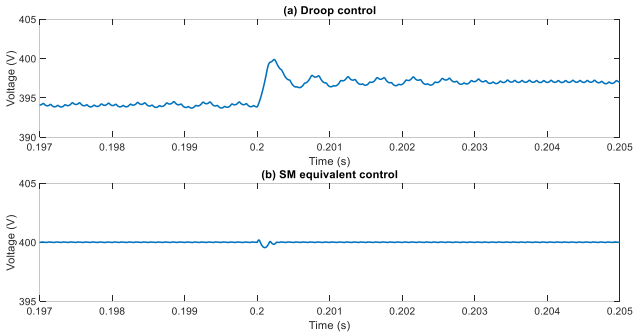

Fig. 11. Voltage when the load is switched from 60 kW to 30 kW at 0.2s

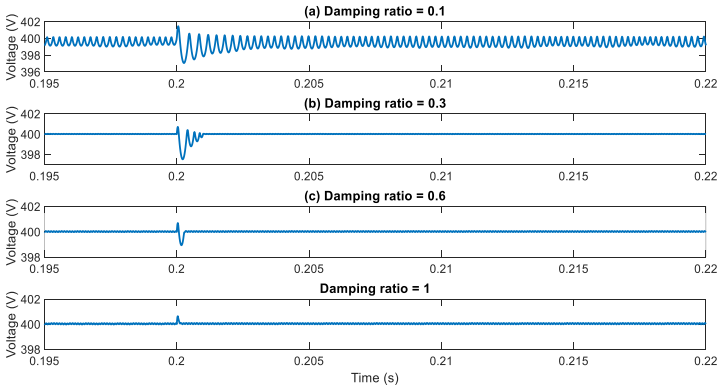

Fig. 12. Dynamic response when the load is switched from 100kW to 60 kW at 0.2s

REFERENCES

Techakittiroj, K. & Wongpaibool, V. 2009. Co-existence between AC-distribution and DC-distribution: in the view of appliances. International Conference on Computer and Electrical Engineering (ICCEE). Dubai, United Arab Emirates.

Yasin, A. R., Riaz, M., Ehab, M. & Raza, A. 2021. Filter Extracted Sliding Mode Approach for DC Microgrids. Electronics. 10(16): 1882. https://doi.org/10.3390/electronics10161882.

Rashad, M., Raoof, U., Ashraf, M. & Ahmed, B. A. 2018. Proportional Load Sharing and

Stability of DC Microgrid with Distributed Architecture Using SM Controller. Mathematical Problems in Engineering. 2018(Article ID 2717129): 16 pages.

Rashad, M., Ashraf, M., Bhatti, A. I. & Minhas, D. M. 2018. Mathematical Modeling and Stability Analysis of DC Microgrid Using SM Hysteresis Controller. Int. Journal of Electrical Power & Energy Systems. 95: 507-522.

Becker, D. & Sonnenberg, B. 2011. DC microgrids in buildings and data centers. IEEE 33rd International Telecommunications Energy Conference (INTELEC).

Hassan, M. A. & He, Y. 2020. Constant Power Load Stabilization in DC Microgrid Systems Using Passivity-Based Control with Nonlinear Disturbance Observer. IEEE Access. 8: 92393-92406. doi: 10.1109/ACCESS.2020.2992780.

Cespedes, M ., Xing, L. & Sun, J. 2011. Constant-power load system stabilization by passive damping. IEEE Trans. Power Electron. 26(7): 1832–1836.

Meng, L., Shafiee, Q., Trecate, G. F. Karimi, H., Fulwani, D., Lu, X. & Guerrero, J. M. 2017. Review on Control of DC Microgrids. IEEE Journal of Emerging and Selected Topics in Power Electron. PP(99):1-1.

Shivam & Dahiya, R. 2017. Robust decentralized control for effective load sharing and bus voltage regulation of DC microgrid based on optimal droop parameters. Journal of Renewable and Sustainable Energy. 9(4): 045301.

Ghalebani, Pedram & Niasati, M. 2018. A distributed control strategy based on droop control and low-bandwidth communication in DC microgrids with increased accuracy of load sharing. Sustainable cities and society. 40: 155-164.

Anand. S., Fernandes, B. G. & Guerrero, J. M. 2013. Distributed control to ensure proportional load sharing and improve voltage regulation in low-voltage DC microgrids. IEEE Trans. Power Electron. 28(4): 1900-1913.

Nasirian, V., Moayedi, S., Davoudi, A. & Lewis, F. L. 2015. Distributed cooperative control of DC microgrids. IEEE Trans. on Power Electron. 30(4): 2288–2303.

Moayedi, S., Nasirian, V., Lewis, F. L. & Davoudi, A. 2015. Team-oriented load sharing in parallel DC–DC converters. IEEE Trans. Ind. Appl. 51(1): 479–490.

Behjati, H., Davoudi, A. & Lewis, F. 2014. Modular DC–DC converters on graphs: Cooperative control. IEEE Trans. on Power Electron. 29(12): 6725–6741.

Morstyn, T., Hredzak, B. & Agelidis, V. G. 2016. Cooperative multi-agent control of heterogeneous storage devices distributed in a DC microgrid. IEEE Trans. on Power Syst., 31(4): 2974–2986.

Karlsson, P. 2002. DC Distributed Power Systems Analysis, Design and Control for a

Renewable Energy System. PhD thesis, Department of Industrial Electrical Engineering and Automation, Lund University, Sweden.

Mahmoodi, M., Gharehpetian, G.B., Abedi, M. & Noroozian, R. 2006. Control systems for independent operation of parallel dg units in dc distribution systems. IEEE International Power and Energy Conf. 220–224.

Dragicevic, T. 2018. Dynamic stabilization of DC microgrids with predictive control of Point-of-Load converters. IEEE Trans. Power Electron. 33(12): 10872-10884.

Fadil, H. E. & Giri, F. 2007. Backstepping based control of pwm dc-dc boost power converters. IEEE International Symposium on Industrial Electron.395–400.

Spiazzi, G. & Mattavelli, P. 2002. Chapter 8: Sliding-mode control of switched-mode power supplies. Power Electronics Handbook,: T.L. Skvarenina (Editor), Boca Raton, FL: CRC Press LLC.

Dominguez, X., Camacho, O., Leica, P., & Rosales, A. 2016. A fixed-frequency Sliding-mode control in a cascade scheme for the Half-bridge Bidirectional DC-DC converter. In Proceedings of the 2016 IEEE Ecuador Technical Chapters Meeting (ETCM). 1–6. Guayaquil, Ecuador.

Etxeberria, A., Vechiu, I., Camblong, H., & Vinassa, J. M. 2011. Comparison of Sliding Mode and PI Control of a Hybrid Energy Storage System in a Microgrid Application. Energy Procedia. 12: 966–974.

Zhao, Y., Qiao, W. & Ha, D. 2014. A Sliding-Mode Duty-Ratio Controller for DC/DC Buck Converters with Constant Power Loads. IEEE Trans. Ind. Appl. 50(2): 1448–1458.

Utkin, V., Guldner, J. & Shi, J. 1999. Sliding Mode Control in Electromechanical Systems. London, U.K.: Taylor and Francis.